Homopolymer Solubilization Limits in Copolymer Micelles: A Monte Carlo Study

M. P. Pépin[†] and M. D. Whitmore*

Department of Physics and Physical Oceanography, Memorial University of Newfoundland, St. John's, Newfoundland, Canada, A1B 3X7

Received December 21, 1999; Revised Manuscript Received August 9, 2000

ABSTRACT: When small concentrations of A-*b*-B diblock copolymer are mixed with A homopolymer or selective solvent, they often form spherical micelles with cores comprised of the B blocks. Simple mean field calculations predict that relatively low molecular weight B homopolymer can be solubilized within the cores, up to a threshold concentration which depends on molecular weight. These predictions are consistent with electron microscopy studies. In this paper, we present a Monte Carlo study of these systems. The results are in qualitative agreement with the phase behavior predicted by mean field theory and observed in the experiments.

1. Introduction

There is great interest in experimental and theoretical studies of polymer blends and solutions. Normally, a binary blend of A and B homopolymers macrophase separates because of the repulsive effective A−B interactions, as described by a positive Flory interaction parameter. The phase-separated blend consists of domains of the minority component dispersed in the majority one. The sizes of the domains depend on the processing history, but typically are on the order of micrometers or larger.

When small amounts of A-*b*-B block copolymer are added to the blend, the copolymers can act as surfactant to disperse the minority component into smaller domains. If there is block copolymer and only one homopolymer (or solvent), e.g., A homopolymer, then the copolymers generally form micelles with the B block of the copolymer forming the core of the micelle and the A block forming a corona. The system of interest in this paper is the A-*b*-B/A/B ternary blend, with only a few percent copolymer and B homopolymer, in a host of A homopolymer or solvent. In this system, one can imagine a number of possibilities, including micelle formation, macrophase separation of the A and B homopolymers, and micelle formation with B homopolymers solubilized within the micelle cores.

A combined experimental and mean field theoretical study of these systems was done by Whitmore and Smith.[1] The theory predicted that, for relatively low molecular weight homopolymer, there exists a threshold volume fraction of homopolymer below which the homopolymer is solubilized within the micelle cores, and above which it macrophase separates. The threshold volume fraction of homopolymer at which the homopolymer macrophase separates, $\phi_{HB}^{(max)}$, depends on the overall volume fraction of the copolymer B block, ϕ_{CB}^{0}, the ratio of the degrees of polymerization of the B homopolymer, Z_{HB}, and the B block of copolymer, Z_{CB}, and the product χZ_{CB} where χ is the Flory interaction parameter for the A and B components in the system. The threshold volume fraction is given approximately by

$$\phi_{HB}^{(max)} \propto \phi_{CB}^{0} (\chi Z_{CB})^{-1/2} \left(\frac{Z_{HB}}{Z_{CB}}\right)^{-3/2} \quad (1)$$

The theoretical results were in qualitative agreement with experiments in which poly(ethylene oxide) (PEO) homopolymer was added to a mixture consisting of PS-*b*-PEO block copolymers in polystyrene (PS) hosts. Transmission electron micrographs (TEM) showed micelle cores ranging in diameter from 20 to 40 nm without added PEO homopolymer and from 20 to 60 nm with a relatively small volume fraction of PEO homopolymer. With a volume fraction of homopolymer well above the predicted threshold, domains ranging up to 400 nm were observed.

Although the mean field approach was successful in describing, at least qualitatively, the solubility limits in such systems, some questions arise about some of the mean field approximations. The solubilization limits are calculated via a simple model of the free energy of the system. In the case of swollen micelles in the strong segregation limit, the density profiles of the copolymer and homopolymer within each micelle are assumed to be uniform, with a sharp core−corona interface, and all micelles are the same size. Also, the B end of each copolymer is assumed to reach the center of the micelles. These assumptions about the structure of the micelles can be investigated with the use of Monte Carlo (MC) simulations. In these simulations, the micelles self-assemble, and no a priori assumptions about the structure of the micelles or their size distributions are required.

Several MC studies[2−14] of block copolymer micelles have been done to study the structure of micelles. Mattice et al.[4−13] have performed several simulations of block copolymer micelles, and studied the effects of added solvent which was compatible with the core-forming block of a triblock-copolymer.[15,16] The studies were done to investigate the effects of added surfactants on stabilizing the domain sizes of the minority solvent component. Although these simulations have been

[†] Current address: Department of Physics, University of Ottawa, 150 Louis-Pasteur, Ottawa, ON, Canada, K1N 6N5.

10.1021/ma992136r CCC: $19.00
Published on Web 10/21/2000

restricted to relatively short polymers, they provide insights into the behavior of these systems.

In this study, we perform MC simulations of block copolymer in solvent with added homopolymer which is compatible with the core-forming block of the micelle. We investigate the structure of the micelles swollen by the homopolymer and the predicted solubilization limits. We revisit the phase behavior predicted by the mean field calculations by investigating the threshold volume fraction of homopolymer and its dependence on the volume fraction and degree of polymerization of the B homopolymer. The techniques developed by Mattice et al. to perform the simulations are used and have been extended to suit this particular type of simulation and gain some understanding of these types of systems. Although the simulations are restricted to relatively low molecular weight polymers, they are used to address questions concerning some of the assumptions in the mean field approach, including the structure and size distribution of micelles, for weakly segregated systems. Our approach includes the calculation of a suite of autocorrelation and diffusion times.

2. Monte Carlo Simulations

Our procedure for performing the MC simulations is described in the previous paper,[14] with the following extensions. These systems contain N_C A-*b*-B copolymers (C) and N_{HB} homopolymers (HB), and the empty lattice sites correspond to solvent (S). The linear dimensions are chosen to accommodate all the polymers with the conditions that the system is large enough to minimize finite size effects, and linear dimension $L > \max(Z_C, Z_{HB})$ where Z_C and Z_{HB} are the numbers of effective monomers for the copolymer and homopolymer, respectively. The homopolymer is the same species as the B block, and the solvent is the same species as the A block. All interactions between like species are set to zero ($\epsilon_{ii} = 0$), and there is only one nonzero effective reduced interaction energy, $\epsilon = \epsilon_{AB}$.

New configurations are generated via the same four types of moves, and accepted or rejected on the basis of the Metropolis[21] rule and excluded volume constraints. Autocorrelation functions, autocorrelation times, and diffusion times are calculated for both copolymer and homopolymer, and the system relaxation time is taken as the maximum of all of them. For the unit of time, one *N*-bead cycle corresponds to $N_C Z_C + N_{HB} Z_{HB}$ Monte Carlo attempts.

It is again useful to describe aggregates in terms of three classifications. We specify "small aggregates" as having 2 or more, but less than 10, polymers. "Micelles" have 10 or more polymers and a size on the order of the molecular dimensions. "Large aggregates" are defined as macrostructures with a large number (typically more than 100) of polymers.

3. Results and Discussion

3.1. Swollen Micelle System. As noted in the Introduction, relatively low molecular weight homopolymer, at low volume fraction, is expected to be solubilized within the micelle cores. In this section, we study a typical system in which solubilization is expected, to probe the assumptions of the mean field model. This system consists of copolymers with $Z_{CB} = 30$ and $Z_{CA} = 42$ and homopolymers with $Z_{HB} = 4$. These relative degrees of polymerization correspond to the experiments of Whitmore and Smith,[1] although their overall values

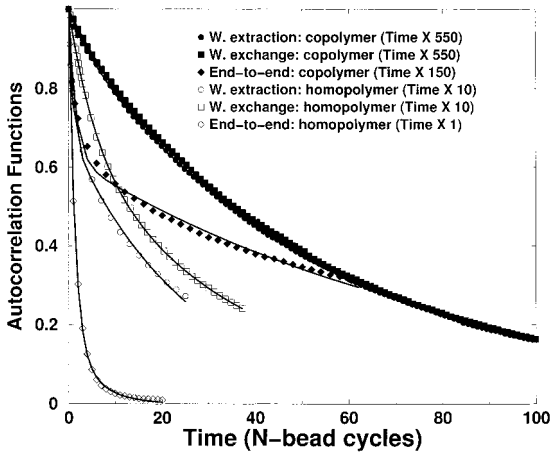

Figure 1. Autocorrelation functions for a system with $\epsilon = 0.31$, $Z_{CA} = 42$, $Z_{CB} = 30$, $Z_{HB} = 4$, $\phi_C = 0.025$, and $\phi_{HB} = 0.0125$: homopolymer-weighted extraction (○), homopolymer-weighted exchange (□); homopolymer end-to-end (◇). The filled symbols correspond to the copolymer autocorrelation functions. The lines are fits to a sum of two exponentials, i.e., Table 1. The functions are plotted on different time scales which are given in the legend.

are much reduced for computational reasons. The overall volume fractions of copolymer and homopolymer are $\phi_C^0 = 0.025$ and $\phi_{HB}^0 = 0.0125$, respectively. The maximum interaction parameter reached was $\epsilon = 0.31$.

Figure 1 shows autocorrelation functions for $\epsilon = 0.31$. They are plotted using different time scales, for convenience. At this value of ϵ, micelles have formed, and the copolymer weighted chain extraction and exchange autocorrelation functions exhibit the slowest decay. The corresponding functions for the homopolymer decay much more rapidly. This reflects the relatively low molecular weight of the homopolymer, and the correspondingly small enthalpic penalty associated with it escaping from an aggregate.

These systems are heterogeneous, with free molecules in solution, small aggregates, and micelles all present. In addition, multiple mechanisms can contribute to each function. Both of these factors can affect the functional forms of the autocorrelation functions. For example, Haliloğlu et al.[22] suggested that there are two main types of mechanisms for the exchange dynamics of copolymers in micelles. The first was referred to as insertion/expulsion (I/E) by which single chains escape micelles and move to other micelles. The second mechanism, which was referred to as merger/splitting (M/S), occurs when the copolymers exchange via micelle cores coming into contact (merger) or when a micelle core splits to form more than one micelle (splitting). Our calculation of the autocorrelation functions does not discriminate between different mechanisms, but incorporates them by averaging over all polymers in the system. All this suggests that the calculated functions can be expressed as a sum of exponentials or stretched exponentials.[23−25] Therefore, we fitted each function to a sum of two exponential functions, i.e.

$$C_s(t) = Ae^{-t/\tau_s} + (1 - A)e^{-t/\tau_l} \qquad (2)$$

where A, τ_s, and τ_l are the fitted parameters. The values are shown in Table 1, and the curves are included in Figure 1. The fitted curves are in reasonably good agreement with the data for all functions. Stretched

Table 1. Results from the Fit of the Autocorrelation Functions to a Sum of Two Exponential Functions, Eq 2[a]

function	A	τ_s	τ_l
copolymer weighted extraction	0.074	5.4×550	56×550
copolymer weighted exchange	0.056	6.2×550	56×550
copolymer end-to-end	0.38	1.5×150	82×150
homopolymer weighted extraction	0.31	0.84×10	26×10
homopolymer weighted exchange	0.36	6.2×10	38×10
homopolymer end-to-end	0.81	1.3×1	5.3×1

[a] The times τ_s and τ_l are given in N-bead cycles for the system with $\epsilon = 0.31$, $Z_{CA} = 42$, $Z_{CB} = 30$, $Z_{HB} = 4$, $\phi_C = 0.025$, and $\phi_{HB} = 0.0125$.

exponential relaxation has also been studied[23,24] in polymer dynamics, and we also fitted Kohlrausch−William−Watts stretched exponential functions[25] of the form $e^{-(t/\tau)^\beta}$. These fits also resulted in good agreement with the data, with values of β varying from 0.39 to 0.93. In contrast, fits to single-exponential functions did not result in good agreement. We note, however, that these fits are done over short time intervals, and a full analysis would require monitoring the functions over a longer time.

The values of the parameter A, which reflect the relative contribution of the "fast" mechanisms, can be qualitatively related to the distributions of the polymers. In this system, about 68% of the homopolymer and 11% of the copolymer are in solution. Hence, we expect processes associated with short autocorrelation times to dominate for the homopolymer, but those associated with long times to dominate for copolymer. For the end-to-end autocorrelation times, the value of A is much larger for the homopolymer than for the copolymer, consistent with this expectation. On the other hand, the weighted exchange and extraction times do not "see" the free polymers, but are calculated only from polymers which are in aggregates of some finite size, with an emphasis on those in the larger aggregates, i.e., the micelles. For these reasons, the values of A do not reflect the proportion of free molecules, but more the distribution between small and large aggregates. For both copolymer and homopolymer, the values of A are smaller than for the end-to-end vector functions, reflecting a smaller qualitative difference between polymers in small vs large aggregates, as compared with the difference between free polymers in solution vs those in aggregates. The larger values of this parameter A for the homopolymer compared to those for the copolymer functions reflect the lower degree of polymerization of the homopolymer. It should be emphasized that although these qualitative ideas are consistent with the numerical results, a quantitative analysis would require a detailed analysis of all mechanisms underlying each function, and this is beyond the scope of this paper. The quantitative results may also be affected by the relative proportion of the different kinds of motions used in the simulations.

Figure 2 shows the autocorrelation times and the times associated with diffusion, as functions of the interaction parameter, ϵ. The times increase with increasing ϵ. The onset of the rapid increase occurs at $\epsilon \simeq 0.28$ where small aggregates and micelles have formed. As the solvent quality decreases, more micelles form, and consequently, the relaxation times and, more specifically, the copolymer-weighted exchange autocorrelation time increase dramatically. The relatively low molecular weight homopolymer can more easily migrate

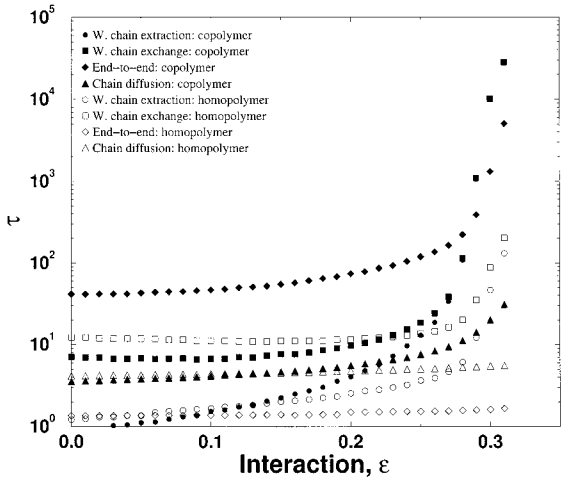

Figure 2. Semilog plot of autocorrelation times as functions of the interaction parameter for the system with $Z_{CA} = 42$, $Z_{CB} = 30$, $Z_{HB} = 4$, $\phi_C = 0.025$, and $\phi_{HB} = 0.0125$: homopolymer-weighted extraction (○); homopolymer-weighted exchange (□); homopolymer end-to-end (◇); homopolymer diffusion (△). The closed symbols correspond to the data for the copolymer.

among aggregates, and more remain in solution. This effect is seen from the homopolymer weighted exchange autocorrelation time which shows a relatively modest increase with increasing ϵ.

At low values of ϵ, there is a considerable difference between the weighted chain extraction and exchange times for both copolymer and homopolymer. This reflects the relatively short time required to escape from an aggregate and the long time to come into contact with another polymer or aggregate.[14] At lower solvent quality, higher ϵ, the opposite is true: the time required to escape from a micelle is much larger than the time needed to migrate to another one. This results in nearly equal chain exchange and extraction times for the copolymer. Also, as aggregates form, the copolymers present in the aggregates become elongated and they can remain oriented for long periods of time, which results in an increase in the end-to-end vector autocorrelation time. In the core of the aggregates, the polymer volume fraction can be high, and both copolymers and homopolymers can remain in the aggregates for extended periods of time. The mobility of the polymers in the aggregates is reduced, and the time associated with the diffusion of polymers increases. At low ϵ, the time associated with the diffusion is smaller than the end-to-end vector autocorrelation times. This is because the polymers are sometimes moved a large distance during a Brownian motion type move.

As ϵ increases, small aggregates (two to nine molecules) begin to form first, as shown in Figure 3. With increasing ϵ, the number of small aggregates first increases, and then micelles begin to form, in this case at $\epsilon \simeq 0.2$ (see inset of Figure 3). Beyond this value of ϵ, the number of small aggregates increases until $\epsilon = 0.27$, and then it decreases. By comparison, the number of micelles increases until $\epsilon = 0.3$. Beyond $\epsilon = 0.3$, the average micelle aggregation number increases, but the number of micelles decreases.

In addition, as ϵ increases, the fraction of polymers in aggregates also increases, as shown in Figure 4. When micelles have formed, the fraction of homopolymer in aggregates is much lower than that of the copolymer, due to the lower molecular weight of these homopolymers.

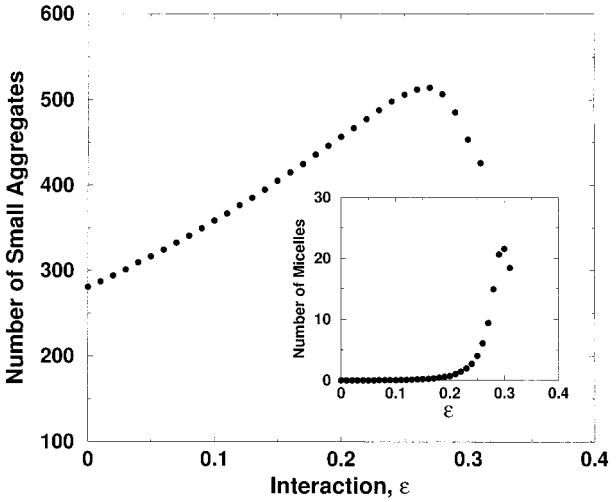

Figure 3. Number of small aggregates in the system as a function of the interaction parameter, ϵ, and number of micelles in the system (inset) as a function of ϵ. A small aggregate is defined as having more than two but less than 10 polymers. A micelle has 10 or more polymers and a well-defined core−corona interface.

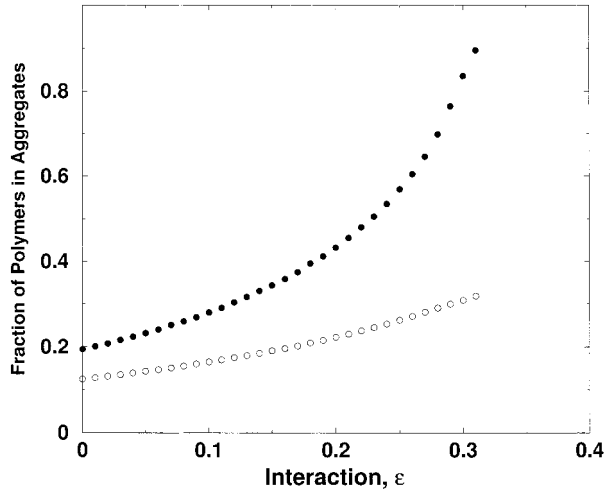

Figure 4. Fraction of polymer in aggregates (small aggregates and micelles) as a function of the interaction ϵ: copolymer (●) and homopolymer (○).

Parts a and b of Figure 5 show the normalized frequency distributions of aggregates as functions of the number of copolymers and homopolymers, respectively, in the aggregates, for this system when $\epsilon = 0.31$. They clearly indicate the presence of free homopolymers and copolymers in solution, small aggregates, and micelles.

Figure 6a shows the volume fraction profiles averaged over micelles with approximately $1135 \pm 7\%$[33] effective monomers (homopolymers and copolymers), which corresponds to approximately the average size of the micelles. The local volume fraction of the copolymer plus that of the homopolymer is as high as 90%. In the core region, the volume fraction profiles for the B copolymer and B homopolymer are quite uniform. This result supports previous experiments[26−29] and theories[30,31] in showing solubilized low molecular weight homopolymer throughout the subdomains. On the other hand, the volume fraction profile in the corona region is nonuniform, as found for the unswollen micelles.[14]

Figure 6b shows normalized distributions of copolymer ends and A−B copolymer joints throughout the micelles. For this figure, the data are collected in bins

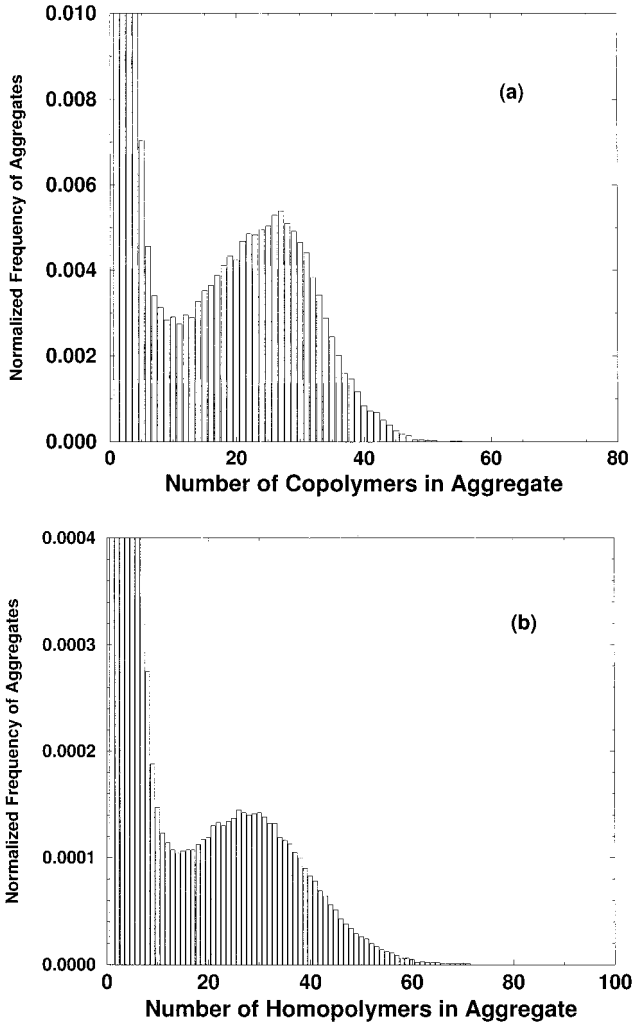

Figure 5. (a) Normalized frequency distribution of aggregates as a function of the number of copolymers. (b) Normalized frequency distribution of aggregates as a function of the number of homopolymers. $\epsilon = 0.31$.

of unit width, in terms of r, which is the distance from the center of mass of the micelle, as described in ref 14. The B copolymer ends penetrate to the center of the micelles, as assumed in the mean field approach but, again, they are distributed throughout the core. The maximum in the distribution of the B ends occurs at $r = 5$. This is consistent with an increase in the number of sites available with increasing r. The inset of Figure 6b indicates a decrease, with increasing r, in the volume fraction of B ends, beyond $r \simeq 5$. However, a local maximum in the distribution of B ends occurs at $r \simeq 16$ in a region of the corona beyond the core−corona interface. This is obviously due to the increased number of available sites, but is nonetheless surprising. The A copolymer ends are distributed throughout the corona, and the A−B copolymer joints are at the core−corona interface. The interface is not sharp, as expected for a weakly segregated system. This relatively weak segregation is also consistent with the fraction of copolymer and homopolymer remaining in solution, 11% and 68%, respectively, as shown in Figure 4.

To summarize, this system shows a distribution of micelle sizes which is similar to diblock copolymer micelles without added homopolymer.[14] The homopolymers are solubilized within the micelle cores, resulting in a microphase consisting of micelles swollen by the

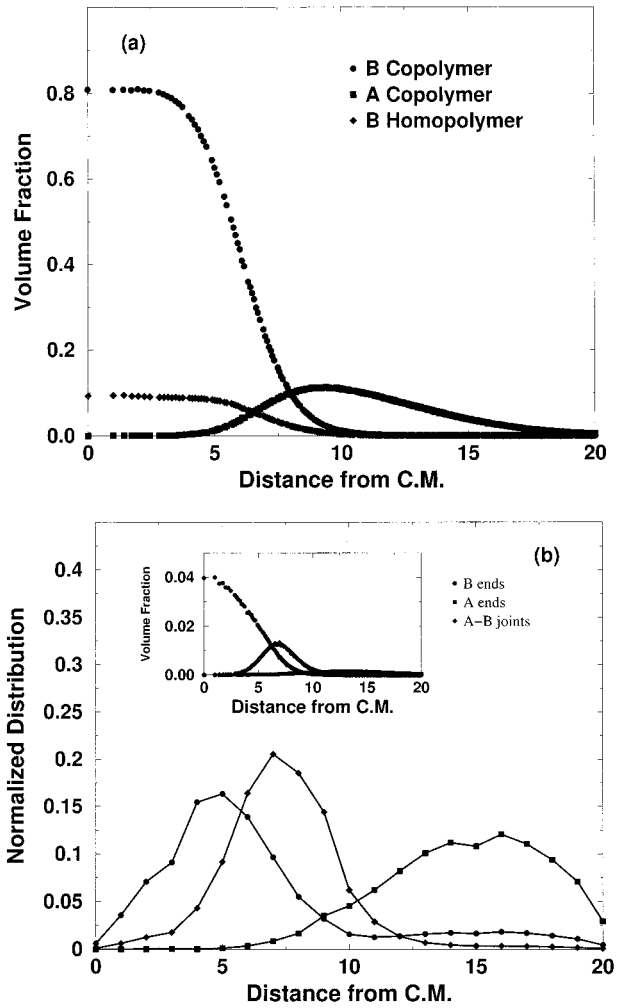

Figure 6. (a) A and B volume fraction profiles as functions of the distance from the center of mass (C.M.) of the micelles. (b) Normalized distributions of A and B copolymer ends and A−B copolymer joints as functions of the distance from the center of mass (C.M.) of the micelles ($\epsilon = 0.31$): B copolymer (●), A copolymer (■), and B homopolymer (◆). The inset shows the volume fraction profiles of A and B ends and A−B joints. The lines are shown as a guide to the eye only.

homopolymer. The densities are approximately uniform within the core, as assumed in the mean field approach, but not in the corona. A considerable fraction of the polymers remains in solution which indicates that this system is not strongly segregated, for interaction energies up to $\epsilon = 0.31$.

3.2. Microphase Separation, Macrophase Separation, and the Solubilization Limit. As discussed earlier, mean field calculations predict a threshold volume fraction of homopolymer below which the homopolymer is solubilized within the micelle cores, and above which the system separates into a macrophase. Furthermore, the theory predicts that this solubilization limit depends on the product χZ_{CB}, ϕ^0_{CB}, and the ratio Z_{HB}/Z_{CB}. In this section, a series of simulations has been done for various ratios of volume fractions and degrees of polymerization to investigate these solubilization limits. In all subsequent simulations, $Z_{CA} = 14$ and $Z_{CB} = 10$. The linear dimensions are chosen such that $L = 80$.

Two simulations are of particular interest. In both, $\phi^0_C = 0.02$ and $Z_{HB} = 6$. In the first one, the homopolymer volume fraction is chosen such that $\phi^0_{HB}/\phi^0_{CB} = 0.1$. In the second one, the homopolymer volume fraction is increased to $\phi^0_{HB}/\phi^0_{CB} = 0.5$. Systems with micelles and homopolymer distributed throughout the micelle cores are identified as microphase-separated. Systems with large aggregates with the homopolymer accumulating at the center and copolymer at the edges are identified as macrophase-separated.

Parts a and b of Figure 7 display snapshots of systems from the first and second simulations, respectively. In Figure 7a, micelles with the homopolymer solubilized in the cores are seen, whereas in Figure 7b, we see a single large domain comprised mostly of homopolymer with copolymers at the interface. This is a macrophase-separated system. In both cases, a significant number of polymers remain in solution and in small aggregates, which indicates a weakly segregated regime.

Figure 8a shows the frequency distribution of aggregates in the first simulation. The micelles have a smooth size distribution with a well-defined peak at about 36 polymers per aggregate. This distribution is once again a signature of a microphase-separated system. In contrast, the domain size distribution shown in Figure 8b for the second simulation shows a single large aggregate with about 800 polymers, which contains about 62% of all polymers in the system.

The volume fraction profiles for the first system are shown in Figure 9a. Once again, the homopolymer is solubilized within the core of the micelles. By contrast, the profiles for aggregates with approximately 800 polymers for the second simulation, shown in Figure 9b, show macrophase separation with homopolymer accumulating at the center of the large aggregate and copolymer at the interface.

Figure 10a shows a semilog plot of the autocorrelation times and the time associated with the diffusion of polymers for the first simulation. [We also did a simulation with $L_i = 100$ and decreasing ϵ. The results showed that finite size effects are negligible, and they were independent of the annealing process.] The general trends shown in Figure 10a for the first simulation are similar to the results shown in Figure 2 but with interesting differences. In this case, micelles and small aggregates first form at a higher interaction energy than the system corresponding to Figure 2, since these are lower molecular weight polymers. This is consistent with mean field theory,[32] which predicts that the critical micelle concentration decreases with increasing χZ_{CB}. A second difference is in the homopolymer weighted extraction and weighted exchange times. In the present case, these times increase with ϵ in concert with the corresponding times for the copolymer. This is due to the higher molecular weight homopolymer, which is now closer to the degree of polymerization of the B block of copolymer. In Figure 10b, where $\phi^0_{HB}/\phi^0_{CB} = 0.5$, the homopolymer weighted extraction and exchange times exceed those of the copolymer. In this case, the aggregating homopolymers form large domains with the copolymers located at the surface, as shown in Figure 7b. The homopolymers therefore remain in the aggregates for extended periods of time. For this macrophase-separated system, the interaction parameter could only be increased up to $\epsilon = 0.42$, due to the large system relaxation time.

The results from these two simulations are consistent with a threshold homopolymer volume fraction, as predicted by mean field theory. Further simulations

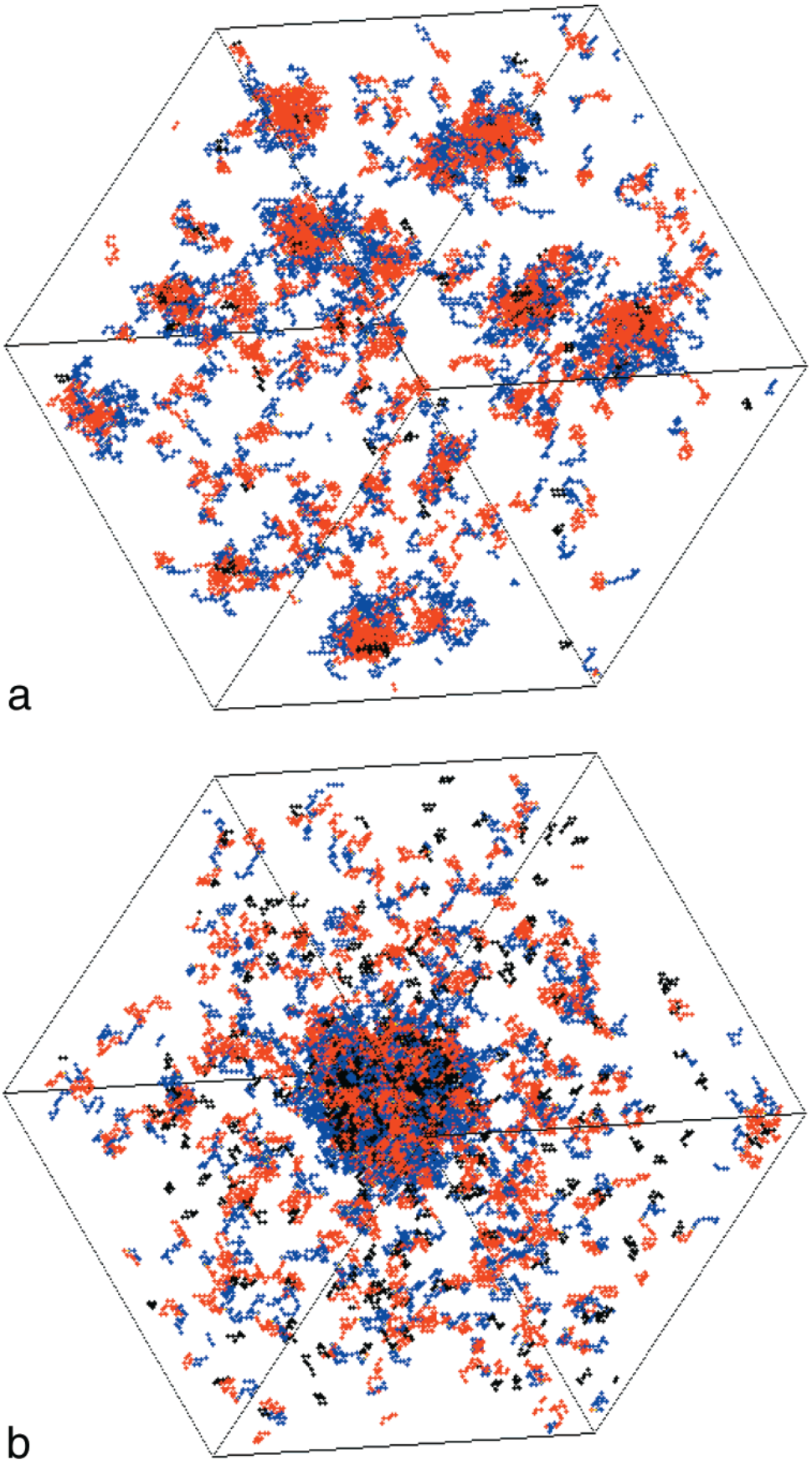

Figure 7. (a) Snapshot of the system with $\phi^0_{HB}/\phi^0_{CB} = 0.1$, $\phi^0_C = 0.02$, $Z_{HB} = 6$, $Z_{CB} = 10$, $Z_{CA} = 14$, $L = 80$, and $\epsilon = 0.49$: A block (blue), B block (red), and B homopolymer (green). (b) Snapshot of the same system except $\phi^0_{HB}/\phi^0_{CB} = 0.5$ and $\epsilon = 0.42$.

were performed to obtain the solubilization limit as a function of the relative volume fractions ϕ^0_{HB}/ϕ^0_{CB} and the ratio Z_{HB}/Z_{CB} by varying the homopolymer volume fraction and degree of polymerization. Figure 11 shows

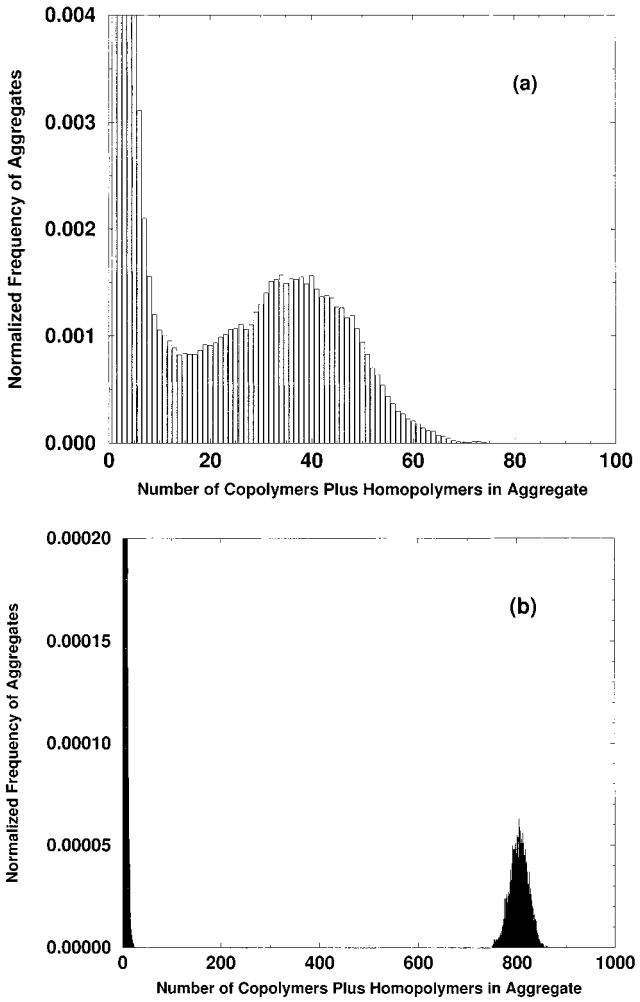

Figure 8. (a) Normalized frequency distribution of aggregates as a function of the number of homopolymers plus copolymers in the aggregates: $\phi^0_{HB}/\phi^0_{CB} = 0.1$, $\phi^0_C = 0.02$, $Z_{HB} = 6$, $Z_{CB} = 10$, $Z_{CA} = 14$, $L = 80$, and $\epsilon = 0.49$. (b) Normalized frequency distribution of aggregates as a function of the number of homopolymers plus copolymers in the aggregates: for the same system except $\phi^0_{HB}/\phi^0_{CB} = 0.5$ and $\epsilon = 0.42$.

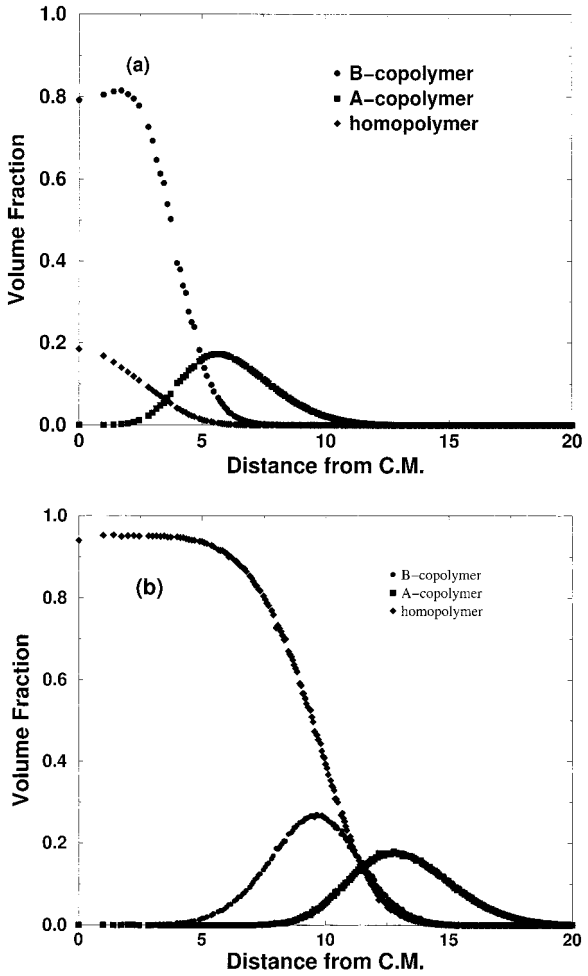

Figure 9. (a) Volume fraction profiles as functions of the distance from the center of mass (C.M.) of the micelles: B copolymer (●), A copolymer (■), and homopolymer (◆), for $\phi^0_{HB}/\phi^0_{CB} = 0.1$, $\phi^0_C = 0.02$, $Z_{HB} = 6$, $Z_{CB} = 10$ and $Z_{CA} = 14$, $L = 80$, and $\epsilon = 0.49$. (b) Volume fraction profiles as functions of the distance from the center of mass (C.M.) of the micelles: for the same system except $\phi^0_{HB}/\phi^0_{CB} = 0.5$ and $\epsilon = 0.42$.

a phase diagram displaying both microphase- and macrophase-separated regions, obtained from these simulations. The open symbols refer to microphase-separated systems, whereas the filled symbols refer to a macrophase. The datum from the simulation in section 3.1 with $Z_{CA} = 42$, $Z_{CB} = 30$, and $Z_{HB} = 4$ is also shown (open circle), even though the interaction parameter could not be increased up to 0.49 as in other microphase-separated systems with $Z_{CB} = 10$; for this case, it could only be increased up to $\epsilon = 0.31$ because of the longer system relaxation time. Nonetheless, the results are consistent with an increase in the threshold volume fraction of added homopolymer with a decrease in Z_{HB}/Z_{CB}. For the macrophase-separated systems, ϵ was increased until the system relaxation time was too large to continue the simulations. In all cases, this occurs when $\epsilon < 0.49$. Nonetheless, since the threshold volume fraction is expected to decrease with increasing ϵ,[14] the macrophase-separated systems are expected to remain macrophase-separated for $\epsilon = 0.49$.

The boundary between the two phases is approximated by the dashed line in Figure 11. This boundary shows that the threshold volume fraction decreases with increasing Z_{HB}/Z_{CB} until only very small amounts of added homopolymer are required to produce a macrophase-separated system. This result is once again consistent with the mean field approach.

4. Summary

We have performed MC simulations of block copolymer micelles swollen by added homopolymer. The simulations were performed by slowly lowering the solvent quality, and carefully monitoring the system characteristics. At each step, autocorrelation functions and their respective times were calculated to determine the required duration of the simulations and to extract information on the dynamic behavior of the systems. This turns out to be important since the system relaxation time is strongly dependent on the solvent quality, and it limits the simulations to low ϵ, i.e., to a weak segregation regime. The simulations therefore serve as a complement to a mean field theory which was developed for strongly segregated systems. In addition, information about the micelle characteristics and other quantities is extracted to investigate approximations made in the mean field approach, and the predictions of the theory on the interplay between the macrophase and microphase separation.

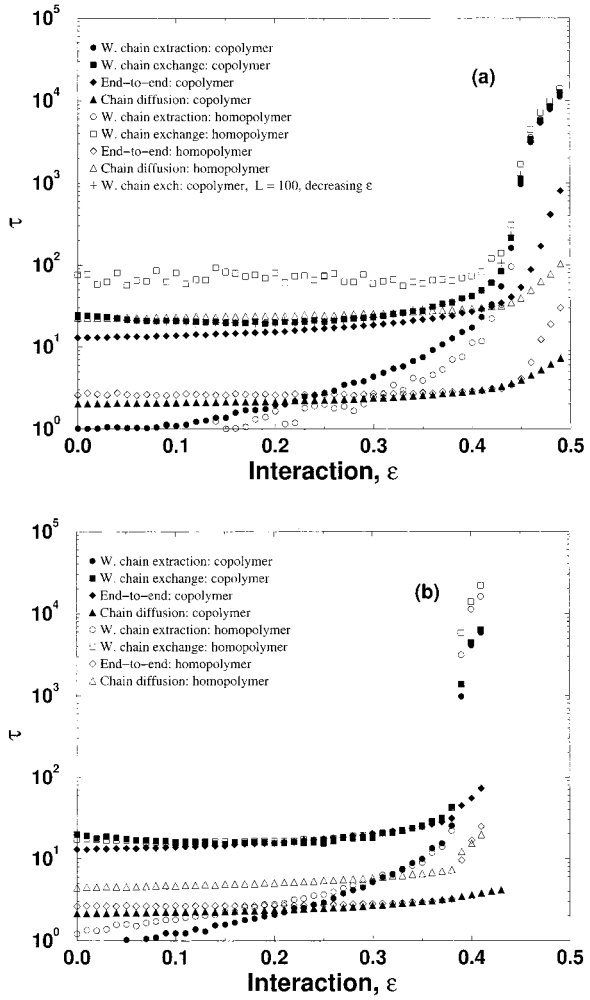

Figure 10. (a) Semilog plot of the relevant autocorrelation times as functions of the interaction parameter: homopolymer-weighted extraction (○); homopolymer-weighted exchange (□); homopolymer end-to-end (◇); homopolymer diffusion (△). The closed symbols correspond to the data for the copolymer. The system is $\phi^0_{HB}/\phi^0_{CB} = 0.1$, $\phi^0_C = 0.02$, $Z_{HB} = 6$, $Z_{CB} = 10$, $Z_{CA} = 14$, $L = 80$, and $\epsilon = 0.49$. (b): As in part a, except $\phi^0_{HB}/\phi^0_{CB} = 0.5$ and $\epsilon = 0.42$.

We detailed the micelle structure for a typical system in which the degree of polymerization of the homopolymer is much smaller than that of the core-forming block of the copolymer, and the homopolymer is solubilized within the micelle cores. The volume fraction profiles in the cores are relatively uniform as assumed in the mean field approach, but in the coronas the profiles are nonuniform. The relatively uniform distributions within the core are consistent with experiments on low molecular weight homopolymer that is solubilized within subdomains.[26−29] The A and B copolymer ends are distributed throughout the coronas and cores of the micelles, respectively, and the joints are localized to a relatively broad interface.

Further simulations were used to study the phase behavior, which was characterized as being microphase- or macrophase-separated. The phase behavior was determined from the volume fraction profiles in the cores of the micelles and from the average size and the size distribution of the aggregates. A threshold volume fraction of homopolymer was identified. Above the threshold, a system is macrophase-separated; otherwise, it is microphase-separated. We also found that the behaviors of the autocorrelation times of the copolymer and homopolymer are related to the phase behavior although a quantitative relationship would depend on knowing the quantitative relationship between the Monte Carlo and real system times.

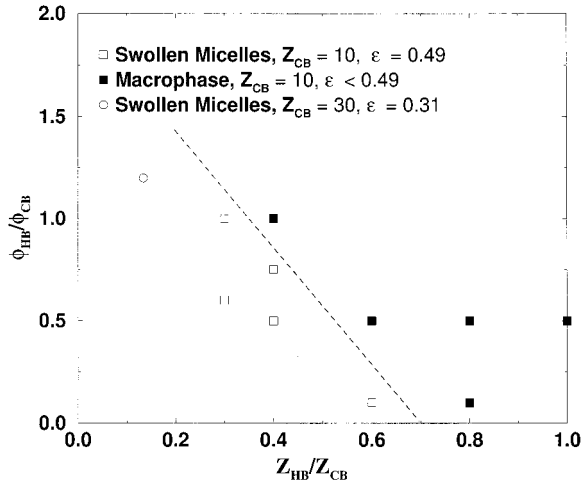

Figure 11. Phase diagram indicating the macrophase and microphase regions as functions of the ratios ϕ^0_{HB}/ϕ^0_{CB} and Z_{HB}/Z_{CB}: microphase-separated (□), macrophase-separated (■), and microphase-separated systems from section 3.1 (○). The dashed line corresponds to the approximate phase boundary.

We obtained a phase diagram which shows that the threshold volume fraction decreases with increasing ratio Z_{HB}/Z_{CB}. This phase behavior and, in particular, the existence of this threshold and its variation with relative degrees of polymerization are in qualitative agreement with the mean field theory.[1] The solubilization of relatively low molecular weight homopolymer and the existence of the threshold are in agreement with experiment, although we are not aware of any experiments that probe the dependence of the threshold on Z_{HB} and Z_{CB}.

In the case of microphase separation, micelles form, the homopolymer is solubilized within the cores, and the aggregates correspond to micelles with reasonably narrow size distributions which are similar to those for unswollen micelles. In the case of macrophase-separated systems, there is a single large aggregate, consisting of homopolymer with copolymer at the surface. The decrease in the threshold volume fraction with increasing Z_{HB} can be attributed to entropic effects: For high molecular weight homopolymer, the entropic penalty in segregating it to a separate macrophase is reduced, so the phase separation occurs at smaller volume fraction.

Acknowledgment. We acknowledge the computing resources offered through Canada's C3.ca program at Université de Montréal, University of Alberta, Unversity of Calgary, and Memorial University of Newfoundland. This work is funded in part by the Natural Sciences and Engineering Research Council of Canada.

References and Notes

(1) Whitmore, M. D.; Smith, T. W. *Macromolecules* **1994**, *27*, 4673.
(2) Bernandes, A. T.; Henriques, V. B.; Bish, P. M. *J. Chem. Phys.* **1994**, *101*, 645.
(3) Molina, L. A.; Freire, J. J. *Macromolecules* **1995**, *28*, 2705.
(4) Haliloğlu, T.; Mattice, W. L. *Polym. Prepr.* **1993**, *34*, 460.
(5) Rodrigues, K.; Mattice, W. L. *Polym. Bull.* **1991**, *25*, 239.
(6) Rodrigues, K.; Mattice, W. L. *J. Chem. Phys.* **1991**, *95*, 5341.
(7) Rodrigues, K.; Mattice, W. L. *Langmuir* **1992**, *8*, 456.

(8) Wang, Y.; Mattice, W. L.; Napper, D. H. *Langmuir* **1993**, *9*, 66.
(9) Zhang, Y.; Mattice, W. L. *Macromolecules* **1994**, *27*, 677.
(10) Rodrigues, K.; Mattice, W. L. *J. Chem. Phys.* **1991**, *94*, 761.
(11) Nguyen-Misra, M.; Mattice, W. L. *Macromolecules* **1995**, *28*, 1444.
(12) Wang, Y.; Mattice, W. L.; Napper, D. H. *Macromolecules* **1992**, *25*, 4073.
(13) Adriani, P.; Wang, Y.; Mattice, W. L. *J. Chem. Phys.* **1994**, *100*, 7718.
(14) Pépin, M. P.; Whitmore, M. D. *Macromolecules* **2000**, *33*, 8644.
(15) Xing, L.; Mattice, W. L. *Macromolecules* **1997**, *30*, 1711.
(16) Xing, L.; Mattice, W. L. *Langmuir* **1998**, *14*, 4074.
(17) Verdier, P. H.; Stockmayer, W. H. *J. Chem. Phys.* **1962**, *36*, 227.
(18) Domb, C. *Adv. Chem. Phys.* **1962**, *15*, 229.
(19) Hilhorst, H. J.; Deutch, J. M. *J. Chem. Phys.* **1975**, *63*, 5153.
(20) Gurler, M. T.; Crabb, C. C.; Dahlin, D. M.; Kovak, J. *Macromolecules* **1983**, *16*, 398.
(21) Metropolis, N.; Rosenbluth, A. W.; Rosenbluth, M. N.; Teller, A. H.; Teller, E. *J. Chem. Phys.* **1953**, *21*, 1087.
(22) Haliloğlu, T.; Bahar, I.; Erman, B.; Mattice, W. L. *Macromolecules* **1996**, *29*, 4764.
(23) Cherayil, B. J. *J. Chem. Phys.* **1992**, *97*, 2090.
(24) Roland, C. M.; Bero, C. A. *Macromolecules* **1996**, *29*, 7521.
(25) Williams, G.; Watts, D. C. *Trans. Faraday Soc.* **1970**, *66*, 80.
(26) Hashimoto, T.; Tanaka, T.; Hasegawa, H. *Macromolecules* **1990**, *23*, 4378.
(27) Tanaka, H.; Hashimoto, T. *Macromolecules* **1991**, *24*, 240.
(28) Tanaka, H.; Hashimoto, T. *Macromolecules* **1991**, *24*, 5712.
(29) Winey, K.; Thomas, E. L.; Fetters, L. J. *Macromolecules* **1991**, *24*, 6182.
(30) Schull, K.; Winey, K. *Macromolecules* **1992**, *25*, 2673.
(31) Banaszak, M.; Whitmore, M. D. *Macromolecules* **1992**, *25*, 2757.
(32) Whitmore, M. D.; Noolandi, J. *Macromolecules* **1985**, *18*, 657.
(33) The entire range of micelle sizes is discretized into 10 intervals, and this defines the number of monomers and the width of the intervals. The interval which includes the maximum in the distribution of micelles is then used for this calculation.

MA992136R